International Journal of Impact Engineering 96 (2016) 35–49

Contents lists available at ScienceDirect

International Journal of Impact Engineering

journal homepage: www.elsevier.com/locate/ijimpeng

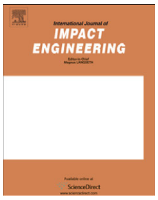

A theoretical study of low-velocity impact of geometrically asymmetric sandwich beams

Jianxun Zhang, Qinghua Qin *, Chunping Xiang, Zhengjin Wang, T.J. Wang

State Key Laboratory for Strength and Vibration of Mechanical Structures, School of Aerospace, Xi'an Jiaotong University, Xi'an 710049, China

ARTICLE INFO

Article history:
Received 13 October 2015
Received in revised form 28 April 2016
Accepted 15 May 2016
Available online 18 May 2016

Keywords:
Sandwich beam
Geometrical asymmetry
Metal foam
Low-velocity impact
Overall bending

ABSTRACT

This paper uses the quasi-static method to investigate plastic behavior of fully clamped geometrical asymmetric sandwich beams with a metal foam core subjected to low-velocity impact. An analytical model is developed to predict the dynamic response of the geometrically asymmetric sandwich beams. Effects of local denting and core strength on the overall bending are considered. Good agreement is achieved between the analytical predictions and numerical results. It is demonstrated that the asymmetric sandwich beams with asymmetric factor $\alpha > 1$ have the larger energy absorption than those with asymmetric factor $0 < \alpha < 1$.

1. Introduction

As a kind of members in the family of lightweight structures, metallic sandwich beams, plates and shells with various cores have received great attention. The sandwich structures are widely used in a number of critical engineering, such as aircraft, spacecrafts, vehicle, etc. The mechanical behavior of sandwich structures depends on the geometries and material properties of the core and face sheets [1]. The conventional sandwich structures have two identical face sheets in material and geometry. However, the face sheets in asymmetric sandwich structures may have different thicknesses and materials, and/or any combination of these. They have different performances and will provide much more choices for the design of structures [2–4].

Over the past decades, attention has been paid on the investigations on impact response of symmetric sandwich structures subjected to low-velocity impacts. Hazizan and Cantwell [5,6] experimentally studied the low-velocity impact response of composite sandwich beams with aluminum honeycomb core and polymer foam core, respectively. Using a simple energy balance model, the maximum impact force and energy absorption capacity were predicted, in which agreement between the energy-balance model and the experimental data was found to be good. Also, the spring-mass model [7–9] were proposed to predict the elastic dynamic response of sandwich structures subjected to low-velocity impact. Li et al. [10] proposed an elastic–plastic model to predict the dynamic response of a simply supported composite sandwich beam when subjected to a mass impact at midspan. Foo et al. [11] modified the energy-balance model to extend its validity to predict the low-velocity impact response of composite sandwich plates beyond the elastic regime. More recently, Qin and Wang [12] obtained the analytical solutions for large deflection response of fully clamped slender metal foam core sandwich beams struck by a heavy mass with the low-velocity, in which local denting is neglected in analysis. Also, Yu et al. [13] experimentally observed the deformation and failure mechanism of low-velocity impact of metal foam core sandwich beams under three-point bending, which is similar to those under quasi-static loading. They found the competing collapse modes, i.e. face yield, core shear and indentation. Vijayasimha et al. [14] experimentally studied the response and energy absorption capacity of cellular sandwich panels that comprise silk–cotton wood skins and aluminum honeycomb core under low-velocity impact loading. Wang et al. [15] experimentally and numerically studied the effects of impactor size, impact energy, face-sheet thickness, and core thickness on the impact behavior of sandwich panels with polyurethane foam core and plain weave carbon fabric laminated face-sheets subjected to low-velocity impact. Zhang et al. [16] experimentally and numerically studied the failure mechanism and structural response of pyramidal truss core sandwich structures consisting of carbon fiber reinforced polymer face sheets and aluminum alloy cores subjected to low-velocity impact, and the numerical results were validated compared with the experimental tests.

In earlier analyses, some research have been devoted to analytically investigating the indentation behaviors of sandwich structures [17–22]. However, the aforementioned analyses were

---

* Corresponding author. State Key Laboratory for Strength and Vibration of Mechanical Structures, School of Aerospace, Xi'an Jiaotong University, Xi'an 710049, China. Tel.: +86 29 82664382; Fax: +86 29 82664382.
E-mail address: qhqin@mail.xjtu.edu.cn (Q. Qin).

http://dx.doi.org/10.1016/j.ijimpeng.2016.05.011

Nomenclature

$2L$	length of the sandwich beam
L_1	distance between the impact point and the left-hand support of the sandwich beam
$L_1^* = \frac{L_1}{L}$	non-dimensional form of L_1
c	thickness of the core
$\bar{c} = \frac{c}{L}$	non-dimensional form of c
h_t	thickness of top face sheet
h_b	thickness of bottom face sheet
$\bar{h} = \frac{h_t + h_b}{2c}$	the non-dimensional form of the thickness of the face sheet
d	diameter of the loading roller
ρ_f	density of the face sheets
σ_f	yield strength of the face sheets
E_f	Young's modulus of the face sheets
E_t	linear strain hardening modulus of the top and bottom face sheets
ν_{ef}	Poisson's ratio of the top and bottom face sheets
ρ_c	density of the metal foam core
σ_c	yield strength of the metal foam core
E_{cf}	Young's modulus of the metal foam core
E_{ct}	linear strain hardening modulus beyond densification of the metal foam core
ν_{ec}	elastic Poisson's ratio of the metal foam core
ν_p	plastic Poisson's ratio of the metal foam core
ε_D	densification strain of the metal foam core
$\bar{\rho} = \frac{\rho_c}{\rho_f}$	relative density of the metal foam core
$\bar{\sigma} = \frac{\sigma_c}{\sigma_f}$	non-dimensional yield strength of the metal foam core
G	mass of the rigid striker
$G^* = \frac{G}{2L(\rho_c c + \rho_f h_t + \rho_f h_b)}$	non-dimensional form of G
ε_c	average compressive strain of the core
α	asymmetric factor
z_p	the location of plastic neutral surface
$\sigma(z)$	yield strength of the material
$\delta = \frac{2\bar{h}(\alpha - 1)}{\bar{\sigma}(\alpha + 1)}$	a dimensionless parameter related to the location of plastic neutral surface
P_c	plastic limit load for the overall bending of the sandwich beam
P_i	plastic limit load for the local denting of the sandwich beam
P	applied load
$P^* = \frac{P}{P_c}$	non-dimensional form of P
P_0	initial load inducing overall bending
$P_0^* = \frac{P_0}{P_c}$	non-dimensional form of P_0
λ	half-length of the local denting deformation
λ_0	initial half-length of the local denting deformation
M'	plastic bending moment of the top face sheet
N'	plastic axial force of the top face sheet
$\dot{e}'$	extension rate of the local denting region of the top face sheet
$\dot{\phi}$	rotation rate of the local denting region of the top face sheet
w_0	deflection induced by local denting at loading point
$w_0^* = \frac{w_0}{h_t}$	non-dimensional form of w_0
$\dot{w}_0$	displacement rate of the local denting region at loading point
$\dot{\varepsilon}$	strain rate of the local denting region of the foam core
W_N	deflection between the plastic neutral surfaces before and after impact at loading point
W_0	deflection induced by overall bending at loading point
$W_0{}^* = \frac{W_0}{c + h_t + h_b}$	non-dimensional form of W_0
W_T	total deflection of the roller
$W_T^* = \frac{W_T}{c + h_t + h_b}$	non-dimensional form of W_T
e	total extension induced by overall bending
e_1	axial extension induced by overall bending concentrated at the end of the left-hand portion
e_2	axial extension induced by overall bending concentrated at the point adjacent to the roller for the left-hand portion
a_1	axial extension induced by overall bending concentrated at the end of the right-hand portion
a_2	axial extension induced by overall bending concentrated at the point adjacent to the roller for the right-hand portion
ψ_1	angular rotation of the left-hand portion

(*continued on next page*)